

## The zebrafish *neckless* mutation reveals a requirement for *raldh2* in mesodermal signals that pattern the hindbrain

Gerrit Begemann<sup>1,\*</sup>, Thomas F. Schilling<sup>2,‡</sup>, Gerd-Jörg Rauch<sup>3</sup>, Robert Geisler<sup>3</sup> and Phillip W. Ingham<sup>1,§</sup>

<sup>1</sup>MRC Intercellular Signalling Group, Centre for Developmental Genetics, University of Sheffield School of Medicine and Biomedical Science, Firth Court, Western Bank, Sheffield S10 2TN, UK

<sup>2</sup>Department of Anatomy and Developmental Biology, University College London, Gower Street, London WC1E 1BT, UK

<sup>3</sup>Max-Planck Institut für Entwicklungsbiologie, Spemannstrasse 36, 72076 Tübingen, Germany

\*Present address: Department of Biology, University of Konstanz, 78464 Konstanz, Germany

‡Present address: Department of Developmental and Cell Biology, University of California at Irvine, Irvine, CA 92697-2300, USA

§Author for correspondence (e-mail: p.w.ingham@sheffield.ac.uk)

Accepted 16 May 2001

### SUMMARY

We describe a new zebrafish mutation, *neckless*, and present evidence that it inactivates retinaldehyde dehydrogenase type 2, an enzyme involved in retinoic acid biosynthesis. *neckless* embryos are characterised by a truncation of the anteroposterior axis anterior to the somites, defects in midline mesendodermal tissues and absence of pectoral fins. At a similar anteroposterior level within the nervous system, expression of the *retinoic acid receptor  $\alpha$*  and *hoxb4* genes is delayed and significantly reduced. Consistent with a primary defect in retinoic acid signalling, some of these defects in *neckless* mutants can be rescued by application of exogenous retinoic acid. We use mosaic analysis to show that the reduction in *hoxb4*

expression in the nervous system is a non-cell autonomous effect, reflecting a requirement for retinoic acid signalling from adjacent paraxial mesoderm. Together, our results demonstrate a conserved role for retinaldehyde dehydrogenase type 2 in patterning the posterior cranial mesoderm of the vertebrate embryo and provide definitive evidence for an involvement of endogenous retinoic acid in signalling between the paraxial mesoderm and neural tube.

Key words: Zebrafish, Anteroposterior patterning, Vitamin A deficiency, Retinoic acid, Retinoic acid receptor, Craniofacial development, Neural crest, *raldh2*, *hoxb4*

### INTRODUCTION

In all vertebrates, inductive cellular interactions result in stable differences in cell states between head, trunk and tail derivatives. In particular, anteroposterior (AP) patterning of the neural tube is regulated by signals from organiser-derived tissues, such as the notochord and prechordal plate, and from paraxial mesoderm (reviewed by Jessell, 2000; Stern and Foley, 1998). Somites clearly influence posterior identities of cells in the neural tube. In heterotopic grafts of hindbrain or somites, neural cells can be respecified to more posterior identities when juxtaposed to posterior mesoderm (Grapin-Botton et al., 1995; Itasaki et al., 1996; Stern et al., 1991). In the posterior head region, putative posteriorising factors have been implicated in patterning both the identities of hindbrain rhombomeres and of neural crest-derived pharyngeal arches (Gould et al., 1998; Muhr et al., 1999; Wendling et al., 2000).

Retinoids are prime candidates for such posteriorising factors since they can have a wide range of effects on AP-patterning in the developing central nervous system (CNS), limbs and neural crest. Exposure of embryos to an excess of retinoic acid (RA) inhibits anterior development in the neural tube and craniofacial mesenchyme through the suppression of

fore- and midbrain-specific gene expression and the expansion of the expression domains of more caudally restricted genes (reviewed by Durston et al., 1998; Gavalas and Krumlauf, 2000). These effects correlate well with the distribution of endogenous RA: both in chick and mouse embryos, RA is detected only after gastrulation with a sharp anterior boundary at the level of the first somite, and at high concentrations caudal to this boundary (Mendelsohn et al., 1991; Rossant et al., 1991; Colbert et al., 1995; Horton and Maden, 1995; Maden et al., 1998). Similarly, in zebrafish the anterior trunk contains high levels of RA (Marsh-Armstrong et al., 1995).

Depriving embryos of RA causes a variety of developmental defects, among them neural crest cell death, the absence of limb buds and posterior branchial arches, small somites, and hindbrain segmentation defects, which collectively are known as vitamin A-deficient (VAD) syndrome (Morriss-Kay and Sokolova, 1996; Maden et al., 1996; Dickman et al., 1997; Maden et al., 2000). In the hindbrain, embryonic RA depletion leads to graded phenotypic effects: with decreasing amounts of RA, expression of genes normally restricted anteriorly progressively extends posteriorly until finally, in the absence of RA signalling, embryos lack rhombomeric and gene expression boundaries posterior to rhombomere 3 (Blumberg

et al., 1997; Dickman et al., 1997; Dupe et al., 1999; Kolm et al., 1997; van der Wees et al., 1998; White et al., 1998; White et al., 2000).

The effects of RA and other retinoids are mediated through nuclear receptors of the RAR and RXR families which act as ligand-activated transcriptional regulators (reviewed by Mangelsdorf et al., 1995). Inactivation of single receptors in mice has revealed extensive receptor redundancy, while compound mutations in some receptors recapitulate the phenotypic defects observed in VAD, including the disruption of AP patterning in the cranial neural crest and hindbrain (Dupe et al., 1999; Kastner et al., 1994; Kastner et al., 1997). These complex phenotypes are not surprising, given the widespread distribution of RA and expression of its receptors. For example, zebrafish *RAR $\alpha$*  and *RAR $\gamma$*  (*rara* and *rarg* – Zebrafish Information Network) expression show little overlap; *RAR $\alpha$*  is expressed in paraxial mesoderm, posterior hindbrain and spinal cord, whereas *RAR $\gamma$*  is expressed more anteriorly in head mesenchyme and in the brain (Joore et al., 1994).

AP patterning of the CNS is mediated through the regulated expression of Hox genes, which are expressed with discrete AP expression boundaries within the developing neural tube and adjacent mesoderm. Binding sites for RA receptors have been characterised in the regulatory regions of *hoxa1*, *hoxb1*, *hoxb4* and *hoxd4*, and shown to confer RA-mediated gene activation in vivo and in vitro, suggesting that RA directly regulates Hox gene transcription (Marshall et al., 1994; Morrison et al., 1996; Dupe et al., 1997; Gould et al., 1998; Studer et al., 1998). Thus, the spatial distribution of RA and its receptors are all thought to be critical for regulating Hox gene expression in the neural tube.

The biosynthesis of RA involves the sequential conversion of vitamin A into retinaldehyde, which is then oxidised to RA. At least two cytosolic alcohol dehydrogenases (ADH), or microsomal retinol dehydrogenases, catalyse the first step, while the second step requires cytosolic retinal dehydrogenases, members of the aldehyde dehydrogenase (ALDH) family (reviewed by Duester, 2000). Two aldehyde dehydrogenases, ALDH1 and ALDH6/V1, are predominantly expressed in spatially restricted domains of the head and retina and are unlikely to contribute to the high levels of RA posteriorly (Haselbeck et al., 1999; Maden et al., 1998). In contrast, retinaldehyde dehydrogenase 2 (RALDH2), a nicotinamide adenine dinucleotide (NAD)-dependent dehydrogenase, is expressed posteriorly in a pattern that correlates with RA-mediated gene activation (Wang et al., 1996; Zhao et al., 1996; Niederreither et al., 1997; Berggren et al., 1999; Swindell et al., 1999). In mouse, loss-of-function mutations in *Raldh2* mimic the most severe phenotypes associated with VAD, implicating *Raldh2* as the main source of RA in the vertebrate embryo (Niederreither et al., 1999; Niederreither et al., 2000).

We have characterised the *neckless* (*nls*) mutation in zebrafish, which recapitulates many aspects of VAD. We link *nls* to a missense mutation in *raldh2*, structural analysis of which predicts a non-functional protein. Consistent with the molecular nature of *nls*, we show that exogenous application of RA rescues the fin and mesodermal defects in *nls* mutants. We also show that zebrafish require *raldh2* for formation of posterior head mesoderm and notochord, as well as for cell specification in the anterior spinal cord. Finally, we show that

the lack of expression of *hoxb4* in the CNS is due to defects in RA signalling from the paraxial mesoderm. Our findings suggest a model in which RA directs AP patterning directly in the mesoderm, and that these cells, in turn, indirectly pattern the neural tube.

## MATERIALS AND METHODS

### Zebrafish husbandry

London wild-type and WIK strains of zebrafish were reared and staged at 28.5°C (Kimmel et al., 1995).

### Mutant screening

Diploid F<sub>2</sub> progeny of male fish mutagenised with ethyl-*N*-nitrosourea (ENU) (Mullins et al., 1994; Solnica-Krezel et al., 1994) from a London wild-type background (Currie et al., 1999) were fixed at 24 hours postfertilisation (hpf) and hybridised with probes for *krox20* (Oxtoby and Jowett, 1993), *pax2* (Krauss et al., 1992), *shh* (Krauss et al., 1993) and *myoD* (Weinberg et al., 1996). In situ hybridisation was performed essentially as previously described (Begemann and Ingham, 2000), using 24-well plates. For double in situ hybridisations, strongly expressed transcripts were labelled with fluorescein and detected with *p*-iodo nitroretazolium violet (INT)/5-bromo-4-chloro-3-indolylphosphate (BCIP), and weakly expressed ones were labelled with NBT/BCIP (Roche Diagnostics).

### Mapping and linkage testing

*nls*<sup>i26</sup> was outcrossed to the WIK strain and the pooled DNA from F<sub>2</sub> homozygous mutants and siblings was analysed using SSLPs. An EST (GenBank Accession Numbers, AI476832 and AI477235) that mapped between z11119 and z8693 on the LN54 radiation hybrid panel (Hukriede et al., 1999), was shown to encode *raldh2* by sequence similarity to other vertebrate *Raldh2* genes. Linkage was determined by RFLP analysis of pooled cDNAs, from 40 'London wild type' and *nls/nls* embryos (oligonucleotides: 5'-AACTGCC-AGGAGAGGTGAAGAACGAC-3' and 5'-ACGGCCATTGCCGG-ACATTTTGAATC-3'). *Pst*I restriction of the amplicates generated a restriction fragment length polymorphism (RFLP) of 0.6 and 0.77 kb in *nls/nls*, and of 1.46 kb in wild type, owing due to a missense mutation in *nls*<sup>i26</sup>.

### Cloning of *raldh2*

Degenerate primers against the peptide sequences IIPWNFP (5'-ATA/C/T ATA/C/T CCI TGG AAC/T TTC/T CC-3') and PFGGFKM (5'-CAT C/TTT A/GAA ICC ICC A/GAA IGG-3') were used to amplify a 0.9 kb *raldh2* fragment by RT-PCR from 30 hours hpf wild-type embryos. Fragments were subcloned into the pCR2.1-vector using the TOPO kit (Invitrogen) and sequenced, revealing one with similarity to vertebrate *Raldh2*. The fragment was screened against a zebrafish late somitogenesis stage cDNA library (Max-Planck-Institute for Molecular Genetics, Berlin) under stringent conditions to obtain a full-length clone of *raldh2* (ICRFp524L2053Q8) (GenBank Accession Number, AF339837). Several cDNAs from different homozygous *nls* mutant embryos and London wild-type embryos were obtained by RT-PCR and sequenced using *raldh2*-specific primers.

### Retinoic acid treatments

Batches of 60–80 embryos from wild-type or *nls* heterozygous parents were incubated in the dark from late blastula stage onwards in varying dilutions (in embryo medium) of a 10<sup>-4</sup> M all-*trans* RA (Sigma)/10% ethanol solution (from a 10<sup>-2</sup> M stock solution in DMSO). As controls, siblings were treated with equivalent concentrations of ethanol/DMSO alone. Mild teratogenic effects (e.g. disrupted heart development and smaller eyes) were observed at higher concentrations.

### mRNA rescue experiments

Full-length RALDH2 cDNA was cloned as a *SpeI/NotI* fragment into the *XhoI* and *NotI* sites of pSP64TXB (Tada and Smith, 2000). The resulting plasmid, pSP64T-RALDH2 was linearised with *XbaI* and transcribed using the 'SP6 mMessage mMachine' kit (Ambion). 3 nl of in vitro synthesised mRNA was injected into embryos at the one- to four-cell stage.

### Morpholino injections

Two partially overlapping morpholinos against *raldh2* (5'-gtt caa ctt cac tgg agg tca tc-3' and 5'-gca gtt caa ctt cac tgg agg tca t-3') were obtained from GeneTools, LLC, and solubilised in water at a stock concentration of 1 mM (8.5 mg/ml). 4-5 nl of 1:2, 1:4 and 1:10 dilutions in water, respectively (approximately 4, 2 and 0.85 mg/ml) were injected into one-cell stage embryos. The injected dilutions resulted in strong (1:2) to weak (1:10) phenocopies of the *nls* phenotype.

### Histology

Cartilage staining was performed as described (Schilling et al., 1996). TUNEL staining for apoptotic cells was performed as described previously (Williams et al., 2000). Labelled DNA was detected with alkaline phosphatase-coupled anti-fluorescein (Roche), followed by a NBT/BCIP (Roche) colour reaction. For live labelling of apoptosis, dechorionated embryos were incubated in 5mg/ml Acridine Orange (Sigma)/1% DMSO/PBS, washed in PBS and observed with a fluorescein filter set. Immunostaining was carried out according to Westerfield (Westerfield, 1995) with antibodies against No tail (Schulte-Merker et al., 1994), myosin heavy chain (Dan-Goor et al., 1990) and the cell-surface protein DM-GRASP (Zn8; Trevarrow et al., 1990). Embryos were cleared in 70% glycerol, mounted on bridged coverslips and photographed on a Zeiss Axioplan microscope.

### Mosaic analysis

Donor embryos were injected at the one-cell stage with 2.5% lysine fixable tetramethyl-rhodamin-dextran and 3.0% lysine fixable biotin-dextran ( $M_r$  100,000)(Molecular Probes) dissolved in 0.2 M KCl. Transplants were done blindly, and donor genotypes determined at 24 hpf. At late blastula stages, groups of 10-30 donor cells were transplanted into unlabelled host embryos of the same stage and placed either along the margins of the blastoderm, which gives rise to the mesoderm, or further away from the margin in regions that give rise to neural ectoderm (Kimmel et al., 1990). Transplanted cells were labelled using a peroxidase-coupled avidin (Vector Labs) and detected with diaminobenzidine (for brightfield microscopy) or a fluorescent tyramide substrate (Renaissance TSA kit; Dupont Biotechnology Systems), and examined for fluorescence.

## RESULTS

### Mutation of the *neckless* gene disrupts posterior head mesoderm and pectoral fin development

The *neckless* (*nls*) mutation was isolated in an in situ hybridisation screen of ENU-mutagenised zebrafish through its effects on gene expression along the AP axis (Fig. 1; Currie et al., 1999). Simultaneous detection of *krox20* expression in the hindbrain and *myoD* expression in somite precursors reveals a reduction in the spacing between rhombomere 5 (r5) and the first somite as early as the tailbud stage in 25% of the progeny of *nls* heterozygotes (Fig. 1G-N). The *nls*<sup>sl26</sup> allele is inherited in a Mendelian fashion as a recessive lethal trait and homozygotes die between 4-6 days postfertilisation. At 18 hpf, the posterior head in mutants is thickened just anterior to the first somite (Fig. 1A,B), and the distance between the otic

**Table 1. Notochord cell count in the head of wild type and *nls***

Phenotype	Sample size (n)	Average number of <i>No tail</i> -expressing cells		
		Rostral to r3	r3-r5	r5-somite 1
Wild type	14	9	73	97
<i>nls</i>	9	11	76	48

Cell numbers expressing the nuclear No tail protein in 10-somite-old embryos, counterstained with *krox20* and *myoD*.

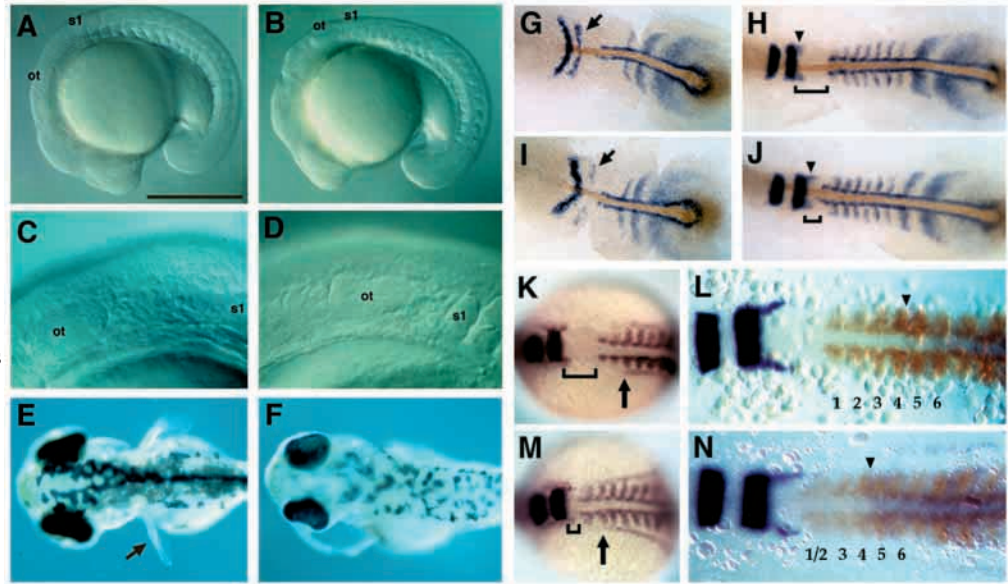
vesicle and the first somite is reduced compared with wild type (Fig. 1C,D). At 30 hpf mutants have weak heartbeats, swollen pericardial cavities and lack apical folds of the developing pectoral fin buds. By 4 days, mutant larvae lack pectoral fins (Fig. 1E,F). Alcian staining of cartilage showed that homozygotes lacked both a pectoral girdle and endoskeletal elements of the pectoral fins (see Fig. 6J). Body shape and fin defects were 100% penetrant in *nls* mutants either in AB or London genetic backgrounds, whereas pericardial swelling had a lower penetrance (data not shown).

To investigate its mesodermal defects further, we compared markers of different mediolateral regions (paraxial, lateral plate and axial). Analysis of *myoD* and *her1* expression revealed no differences in the length of the somitic plate, or number of somites formed, in *nls* homozygotes (Fig. 1G-J). The nephric tubules, which derive from lateral plate mesoderm and express *pax2*, are invariantly located lateral to somite 3 in *nls*, as in wild type (Fig. 1K,M). By contrast, *nls* mutants have fewer notochord cells, visualised using an anti-No tail antibody in the posterior head (Fig. 1G-J; see Table 1). At 12 hpf the number of No tail-positive cells between r5 and somite 1 is reduced by approximately 50% in *nls* (Table 1). The number of developing anterior somites is unchanged, as expression of *hoxc6* is detected up to the boundary between the fourth and fifth somites in *nls* as in wild type (Molven et al., 1990; Prince et al., 1998a). Thus, *nls* mutants exhibit early defects in both paraxial and axial mesoderm in the region that will form the posterior head and pectoral fins.

### A mutation in *raldh2* co-segregates with *nls*

Using bulked segregant analysis we mapped *nls* between SSLPs z11119 and z8693 on LG7 (Fig. 2B,C). This location coincides with that of an EST predicted to encode a close relative of mammalian *Raldh2*. As the *nls* phenotype shows some similarities to that of VAD quail and *Raldh2* mutant mouse embryos, *Raldh2* seemed a good candidate for the *nls* gene. We sequenced a full-length cDNA encoding zebrafish *raldh2* (Fig. 2A) and six independent isolates of RALDH2 cDNAs from homozygous *nls* embryos that all contain a point mutation (Gly204Arg) (Fig. 2D). This creates a fortuitous *PstI* restriction site with which we confirmed linkage to *nls* by RFLP analysis (Fig. 2E). Glycine 204 is one of 23 residues that are invariant among 16 NAD and/or NADP-linked aldehyde dehydrogenases with wide substrate preferences, as well as types with distinct specificities for metabolic aldehyde intermediates, particularly semialdehydes (Perozich et al., 1999) and forms the core of a loop-forming sequence motif that lies within the NAD-binding domain of the molecule. Modelling the structural effects of substituting glycine 204 with arginine by comparison with the tertiary structure of rat RALDH2 (Lamb and Newcomer, 1999)

**Fig. 1.** Mesodermal and fin defects in *nls* mutant embryos. (A,B) Lateral views of living 17-somite stage wild-type (A) and *nls* mutant (B) embryos, photographed with Nomarski optics, showing a kink at the head-trunk boundary in *nls*. (C,D) Higher magnification view of the posterior head, showing proximity of the first somite to the otic vesicle in *nls* (D). (E,F) Dorsal views of living 4-day-old wild-type (E) and *nls* mutant (F) larvae showing absence of pectoral fins (arrow) in *nls*. (G-N) Dorsal views of embryos labelled with in situ hybridisation and flat-mounted to show reduction in the distance between the *krox20* and *myoD* expression domains (brackets) between *nls* mutants (I,J,M,N) and wild types (G,H,K,L). (G-J) Immunohistochemical co-localisation of the No tail protein (brown) with *krox20*, *myoD* and the presomitic marker *her-1* in *nls* mutants. At the five-somite stage (G,I), expression of *krox20* is slightly delayed in rhombomere (r) 5 (arrows). At the 10-somite stage (H,J), posterior head defects in *nls* are more pronounced and *krox20* expression in r5 has recovered. Arrowheads denote migrating neural crest cells from r5 that appear normal in *nls*. (K,M) Co-localisation of the pronephric marker *pax2* reveals that its anteriormost extension in the lateral mesoderm is located lateral to somite 3 in both wild type and *nls* (arrows). (L,N) Co-localisation of *hoxc6* (purple) with *krox20* and *myoD* (brown) at the ten-somite stage reveals an anterior limit of *hoxc6* expression at the somite 4/5 boundary in both wild type and *nls* (arrowheads). Note the loss of clear separation between the first two somites in *nls* (N). Ot, otic vesicle; s1, somite 1. Anterior is towards the left. Scale bar: 500  $\mu$ m in A,B.



suggest that this mutation prevents a secondary structure that allows interaction of the protein with the co-enzyme NAD (data not shown). Owing to the tight spacing of glycine 204 within its surroundings, replacing this residue with arginine appears to be sterically prohibitive and would create a protein of reduced or no activity.

### Morpholino-mediated translational inhibition of RALDH2 phenocopies *nls*

To investigate whether loss of RALDH2 activity could account for the *nls* phenotype, we injected *raldh2*-specific morpholino antisense oligonucleotides into wild-type embryos and assayed the ensuing effects by in situ hybridisation with appropriate marker probes. Injection of either 8.5 or 17 ng of the *raldh2*-morpholino resulted in a strong reduction in the space between the *krox20* and *myoD* expression domains at 12 hpf relative to wild type (Fig. 3A), a phenotype indistinguishable from that of *nls*<sup>i26</sup> embryos at the same stage (Fig. 1I). On average, 71 out of 101 embryos injected with both concentrations and either morpholino exhibited this phenotype. Moreover, distinct rhombomeres r3 and r5 can be observed in the injected embryos. At 24 hpf, the post-otic head is shortened and *tbx5* expression in the pectoral fin buds is abolished (not shown). We never observed phenotypes stronger than those exhibited by *nls*<sup>i26</sup> homozygotes, indicating that the *nls*<sup>i26</sup> mutation is equivalent to the loss of RALDH2 activity. Injection of 34 ng *raldh2*-morpholino did, however, cause neural necrosis, which we interpret to be a nonspecific effect.

### Exogenous RA or RALDH2 activity rescues aspects of the *nls* mutant phenotype

As RALDH2 catalyses the last step in the synthesis of all-

*trans*-RA, the main constituent of retinoids in zebrafish embryos (Costaridis et al., 1996), we investigated whether or not exogenous RA can rescue the mesodermal and fin defects caused by *nls*. Two early fin markers, *tbx5.1*, which labels the entire pectoral fin field (Begemann and Ingham, 2000), as well as *shh*, a marker of posterior fin mesenchyme (Krauss et al., 1993), are undetectable in the presumptive fin mesenchyme of *nls* homozygotes (Fig. 3C,E,G-I). Exposure to all-*trans*-RA rescued caudal head mesoderm development at 12 and 17 hpf (Fig. 3B; Table 2), as well as the pectoral fin expression of *tbx5.1* at 36 hpf (Fig. 3J,L), consistent with the *nls* mutation causing a reduction or loss of RA signalling.

To confirm that the molecular lesion in *nls/raldh2* is responsible for the *nls* mutant phenotype, we injected in vitro transcribed *raldh2* mRNA into one- to four-cell *nls* embryos and assayed for the rescue of *tbx5.1* expression in the pectoral fin buds, as well as for development of an apical fin fold. The concentration of injected *raldh2* mRNA was progressively reduced until overexpression phenotypes, similar to those observed in RA-treated embryos, were no longer observed. This concentration (approx. 500 pg per embryo) was used to assay phenotypic rescue in batches of embryos derived from a cross between *nls*-heterozygotes (Table 3). Partial or complete restoration of *tbx5.1* expression was seen in 83% of mutants (30/36 expected *nls* embryos), indicating that wild-type *raldh2* is sufficient to rescue *nls* embryos.

### *nls/raldh2* is expressed in early trunk paraxial mesoderm

To investigate the spatial and temporal patterns of *nls/raldh2* expression during embryogenesis, we used whole-mount in situ hybridisation. *raldh2* mRNA is first detectable at 30%

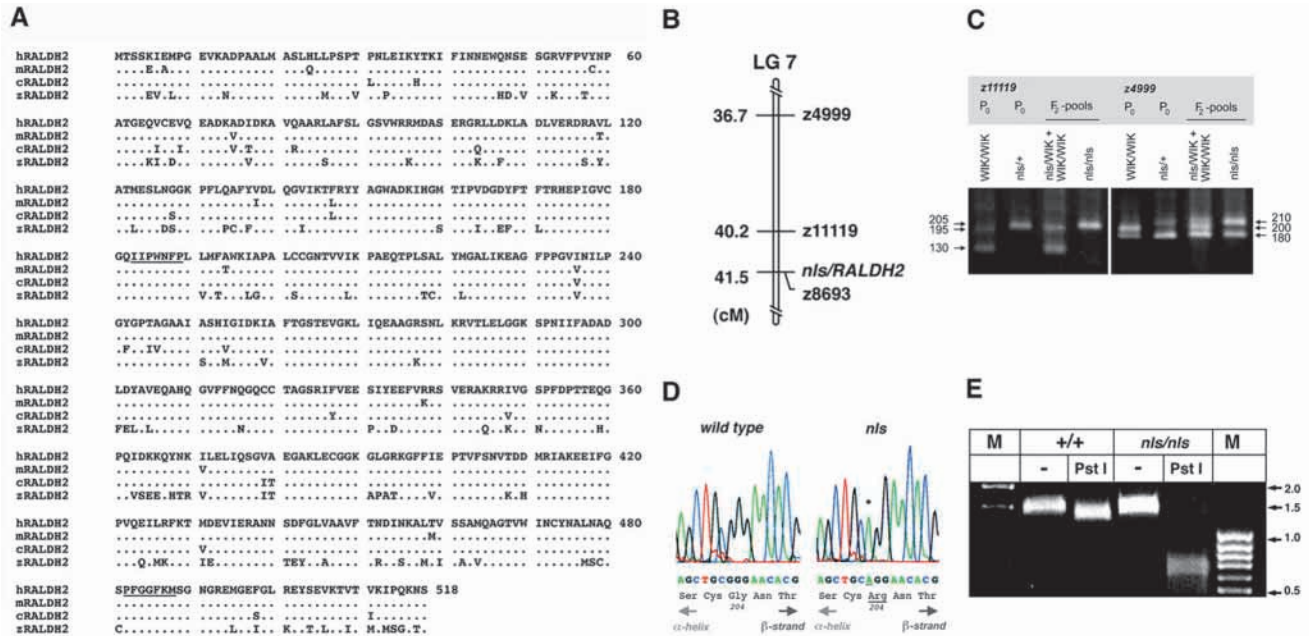


**Fig. 2.** Cloning and mapping of zebrafish *nls/raldh2*. (A) Comparison of the predicted RALDH2 amino acid sequence of human (Accession Number, O94788), mouse (Q62148), chick (O93344) and zebrafish proteins. Zebrafish RALDH2 protein has 79% amino acid identity and 91% similarity to the human protein. Sequence conservation within the first 20 amino acids suggests that RALDH2 proteins may be translated from the first methionine, rather than methionine 20; the 19 N-terminal amino acids for the mouse and chick proteins were derived from their cDNA sequences. Underlined sequences correspond to primers used for RT-PCR cloning. Alignment was performed using PILEUP. (B) Schematic of part of linkage group 7 (LG7), showing the *nls/raldh2* map position in relation to SSLP markers. Data were combined with those from the meiotic and LN54 radiation hybrid panels to determine the position of the *raldh2* EST and *nls*. (C) Linkage analysis with SSLP primers on genomic DNA from *nls*, outcrossed to the WIK strain. In parental strains, primer pair z11119 amplified a single band of 205 base pairs (bp) in the heterozygous *nls* carriers and two bands of 195 bp and 130 bp, in WIK. In F<sub>2</sub> progeny, these primers amplified the 205 bp fragment in only homozygous *nls/nls* embryos, demonstrating linkage to this marker. Likewise, SSLP marker z4999 amplifies a fragment of 210 bp in heterozygous *nls/+* parents, and a fragment of 200 bp in WIK (a fragment of 180 bp is amplified in both strains). These primers amplified only the 210 bp fragment in pools of homozygous F<sub>2</sub> *nls* embryos, whereas sibling embryos contained both fragments. Thus, *nls* is closely linked to SSLP markers z11119 and z4999, and to z11894 and z8693 (not shown, see Materials and Methods). (D) A single point mutation in all of six independently subcloned cDNAs within the *nls* open reading frame, generates a missense mutation of Gly<sup>204</sup> to Arg<sup>204</sup> (asterisk), located in a loop structure. (E) *Pst*I restriction of PCR-fragments, amplified using *raldh2*-specific primers, of cDNA pools of 40 London wild-type (+/+) and *nls/nls* embryos, respectively, generates RFLPs of 0.6 and 0.77 kb in *nls/nls*, and of 1.46 kb in wild type. M, molecular weight marker.

**Table 2. Pharmacological rescue of *nls* embryos by RA treatment**

**A. Rescue of pectoral fin development\***

Concentration (M) and sample size (n)	RA treated			Control (DMSO/ethanol-treated)	
	Wild type	<i>nls</i>	Sample size (n)	Wild type	<i>nls</i>
10 <sup>-9</sup> (n=122)	91 (75%)	31 (25%)	n=56	48 (86%)	8 (14%)
10 <sup>-8</sup> (n=126)	97 (77%)	29 (23%)	n=59	41 (69.5%)	18 (30.5%)
10 <sup>-7</sup> (n=115)	104 (92%)	11 (8%)	n=54	39 (72%)	15 (28%)
10 <sup>-6</sup> (n=56)	53 (94%)	3 (6%)	n=59	40 (68%)	19 (32%)

**B. Rescue of caudal head mesoderm‡**

10 <sup>-6</sup> (n=56)	55 (98%)	1 (2%)	n=59	46 (78%)	13 (22%)
5×10 <sup>-7</sup> (n=55)	55 (100%)	0 (0%)	n=53	42 (79%)	11 (21%)

\*Treated embryos were classified at 36 hpf for the presence (wild type + rescued *nls*) or absence (*nls*) of pectoral fin buds. Embryos from a wild type cross-treated under identical conditions did not show alterations to pectoral fins upon RA treatment.

‡Embryos were classified by in situ hybridisation at 12 hpf (10<sup>-6</sup> M) and 17 hpf (5×10<sup>-7</sup> M) for distance between *krox20* and *myoD* expression. In all experiments, teratogenic effects were observed when treated with 10<sup>-6</sup> M RA.

epiboly in an open ring along the blastoderm margin (Fig. 4A). Upon gastrulation, *raldh2* is expressed in involuting cells at the margin that will form mesendoderm (Fig. 4B,C), but is excluded from the most dorsal cells of the embryonic shield.

Expression persists in posterior and lateral mesoderm during gastrulation and remains excluded from notochord precursors (Fig. 4D). By 15 hpf, expression is found in forming somites, as well as in lateral plate mesoderm extending into the cranial

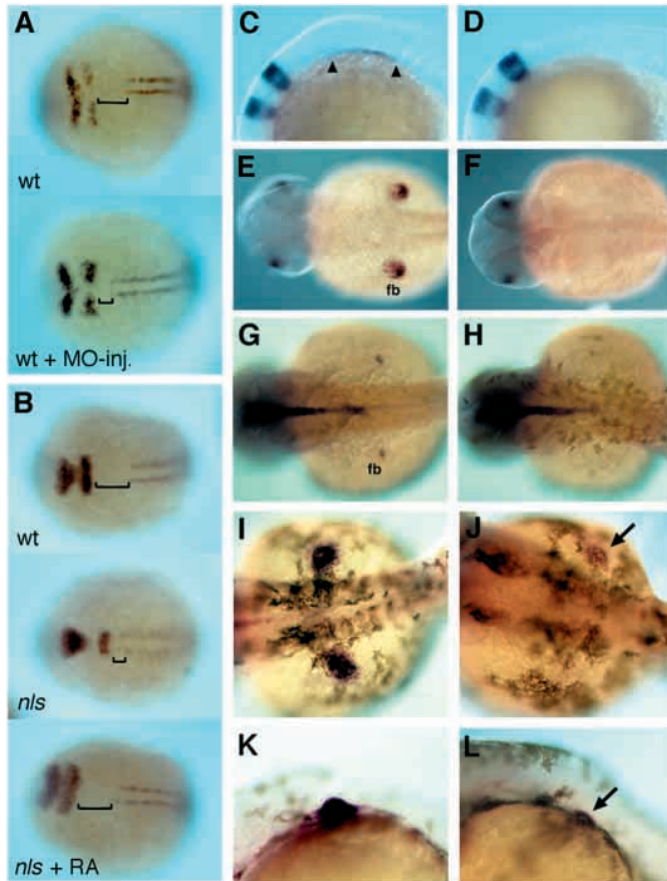


**Fig. 3.** *raldh2* morpholino induced phenocopies and rescue of mesodermal and pectoral fin development in *nls* through RA application. (A,B) Expression of *krox20* and *myoD*, dorsal views. (A) Injection of a *raldh2*-morpholino into wild-type phenocopies the mesodermal defects in *nls*. (B)  $10^{-6}$  M RA rescues mesoderm development in *nls* (12 hpf); brackets indicate the postotic head. (C-L) Wild-type (middle panels) and *nls* (right panels) embryos in dorsal (E-J) or lateral (C,D,K,L) view, anterior towards the left. (C-F) In situ hybridisation reveals an absence of *tbx5.1* expression, which marks forelimb mesoderm, in *nls* at the 12-somite stage (C,D), as well as later during fin outgrowth at 28 hpf (E,F). (G,H) At 32 hpf, *shh* expression, a marker for posterior fin mesenchyme, is absent in *nls* embryos. (J,L) 36 hpf,  $10^{-7}$  M RA rescues *tbx5.1* expression in *nls* pectoral fin buds (arrow); rescued fin buds often develop apical folds (L, arrow), although never as progressed in growth as in wild-type siblings.

region and in the pronephric anlage (Fig. 4E). Somite expression persists throughout segmentation (Fig. 4F,G,I,J) becoming progressively restricted to the somite periphery. By 32 hpf, *nls/raldh2* is expressed in subsets of the pharyngeal arch mesenchyme adjacent to the otic vesicle (Fig. 4H,K) and in the posterior mesenchyme of the forming pectoral fins (Fig. 4N). Other sites of expression are the endoderm (not shown), cells in somites 1-3 adjacent to the notochord and spinal cord (Fig. 4L), the dorsal retina and choroid fissure (Fig. 4O), and motoneurons that innervate the pectoral fins (Fig. 4M and data not shown). Surprisingly, we found that in *nls* embryos the expression of *nls/raldh2* is upregulated in somites and in the cervical mesoderm that flanks the posterior hindbrain (Fig. 4P-S), whereas expression is absent in structures that are reduced in the mutant (see below).

### Craniofacial skeletal and muscle defects in *nls*

To determine the later consequences of the embryonic patterning defects in *nls* for larval development, we examined skeletal and muscle anatomy. In all vertebrates, cells of the cranial mesoderm give rise to the pharyngeal and limb musculature (Noden, 1983; Schilling and Kimmel, 1994), which express the myogenic marker myosin heavy chain (Fig. 5A-D). In zebrafish larvae at 72 hpf, pharyngeal muscles can be identified by their segmental attachments and positions along the dorsoventral axis within each pharyngeal arch (Schilling and Kimmel, 1997). *nls* mutants develop normal patterns of muscles in the first two arches, the mandibular and hyoid, as well as extraocular muscles, while muscles of the five branchial arches (i.e. dorsal pharyngeal wall muscles, rectus ventralis, transversus ventralis), which derive from posterior head mesoderm, are absent (Fig. 5B,D). Consistent with the molecular data indicating that the identities of anterior somites are unaffected in *nls*, we found that the sternohyal muscles, which are thought to originate from myoblast populations within the somites 1-3 (Schilling and Kimmel, 1997), are present (Fig. 5D).

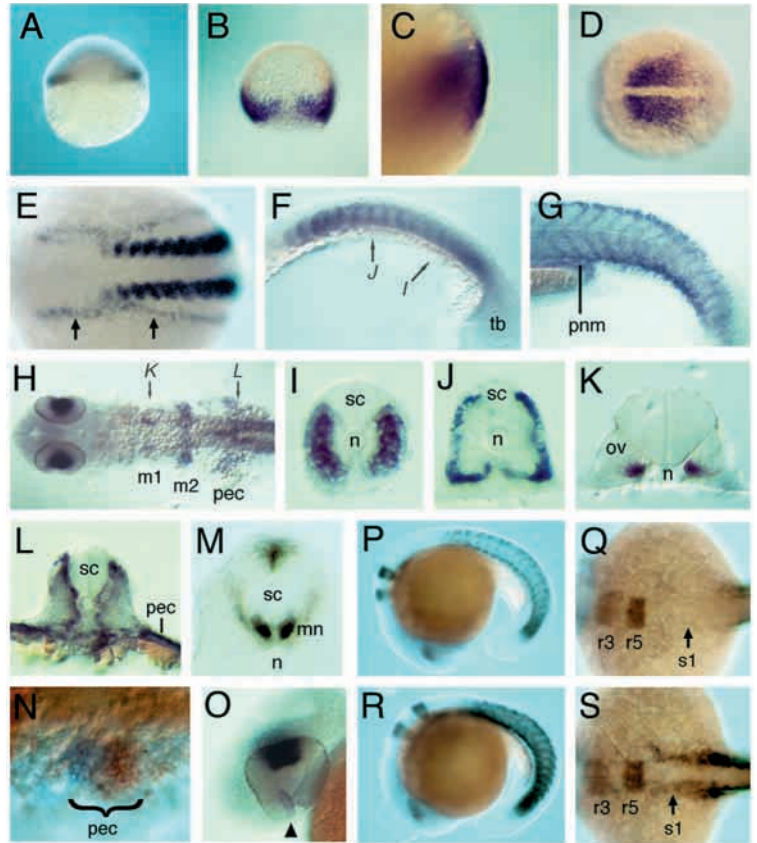
Defects in the branchial musculature in *nls* mutants correlate with defects in the neural crest-derived head skeleton, which can also be identified by their segmental locations (Fig. 5E,F). Alcian Blue staining showed that cartilages of the mandibular and hyoid arches are present in *nls*, though reduced in size compared with wild type. In contrast, skeletal elements in the branchial arches are reduced or absent (from dorsal to ventral these include the ceratobranchials and hyobranchials in arches

**Table 3.** Injection of *RALDH2* mRNA rescues *tbx5.1* expression in *nls*

Experiment	Total number of embryos	Number of observed phenotypes		
		Wild type (% of total)	Weak expression (% of total)	No expression (% of total)
A	40	29	6	5
B	21	13	7	0
C	45	38	7	0
D	40	32	7	1
Sum	146 (100%)	112 (77%)	27 (18%)	6 (4%)
Theoretically expected	146 (100%)	110 (75%)	0	36 (25%)

Microinjection of *RALDH2* mRNA into the progeny of *nls*/WIK heterozygous parents. Selected embryos with missing or partial expression of *tbx5.1* in the pectoral fin buds was assayed at 24 hpf. Putatively rescued animals were genotyped and confirmed as being *nls* homozygotes using SSLP markers. Expression in pectoral fins was assayed as 'weak' when less strong than retinal expression in the same specimen. Percentages rounded to the nearest 1%. Uninjected batches were kept as controls.

**Fig. 4.** Expression of *raldh2* in wild-type and *neckless* embryos. (A–O) In situ hybridisation to detect *raldh2* mRNA in wild types. (A) Expression in marginal cells at 30% epiboly. (B) Dorsal view showing expression in the germ ring of the gastrula at 70% epiboly and absence of dorsal expression. (C) Lateral view at 85% epiboly, showing expression in deep, involuted cells of the hypoblast. (D) Dorsal view at tail bud stage showing expression in the presomitic mesoderm. (E) Dorsal view at the 12-somite stage showing expression in somites and lateral plate mesoderm (arrows). (F) Lateral view at 17 hpf showing expression in the anterior of each somite (arrows denote levels of sections in I,J). (G) Lateral view at 32 hpf, showing expression at somite boundaries, dorsal and ventral somite extremities, and pronephric mesoderm (pnm). (H) Dorsal view at 32 hpf, showing expression in the eyes and in mesenchyme flanking the otic vesicle (m1 and m2), pectoral fin buds (pec) and somites (arrows denote levels of sections in K,L). (I–M) Transverse sections at 17 hpf (I,J), 32 hpf (K,L) and 60 hpf (M), showing expression in the distal myotome but not adaxial cells (I, somite 14-level) (n, notochord), in the periphery of mature somites (J, somite 7 level), adjacent to the otic vesicle (ov) (K), and in pectoral fin and somitic mesoderm adjacent to the spinal cord (sc) (L, somite 3 level). (M) Expression in ventral motoneurons (mn) and dorsal spinal cord neurons at pectoral fin level. (N) Dorsolateral view at 30 hpf, showing expression in posterior pectoral fin buds (blue), double-stained for *tbx5.1* (orange). (O) Lateral view at 33 hpf showing expression in the dorsal retina and anterior to the choroid fissure (arrowhead). (P–S) Co-localisation of *krox20* and *raldh2* at 19 hpf in wild types (P,Q) and in *nls* (R,S). (P,R) Lateral views showing upregulation of somitic expression in *nls* embryos, (Q,S) Dorsal views of same embryos showing upregulated *raldh2* expression in lateral plate mesoderm in *nls* mutants (arrows); broadened *krox20* expression in the hindbrain distinguishes *nls* from wild-type embryos.



4–7, and an axial row of basibranchials in arches 4 and 5) whereas these elements are still present in branchial arch 1. The expressivity of this phenotype is dependent on the genetic background, so that in individual outcrossed lines of *nls*<sup>si26</sup> all five branchial arches may be deleted. All cartilage elements of the pectoral skeleton are also consistently absent. The defects in branchial arch morphogenesis in *nls* are mirrored by the lack of formation of endodermally derived pharyngeal pouches that form the prospective gill slits (Fig. 4G,H). Thus, the early defects at the head/trunk boundary during somitogenesis in *nls* correlate with later defects in the formation of tissues derived from all three germ layers in the pharyngeal segments as well as the pectoral fins that form in this location.

### Neural crest defects in *nls* mutants

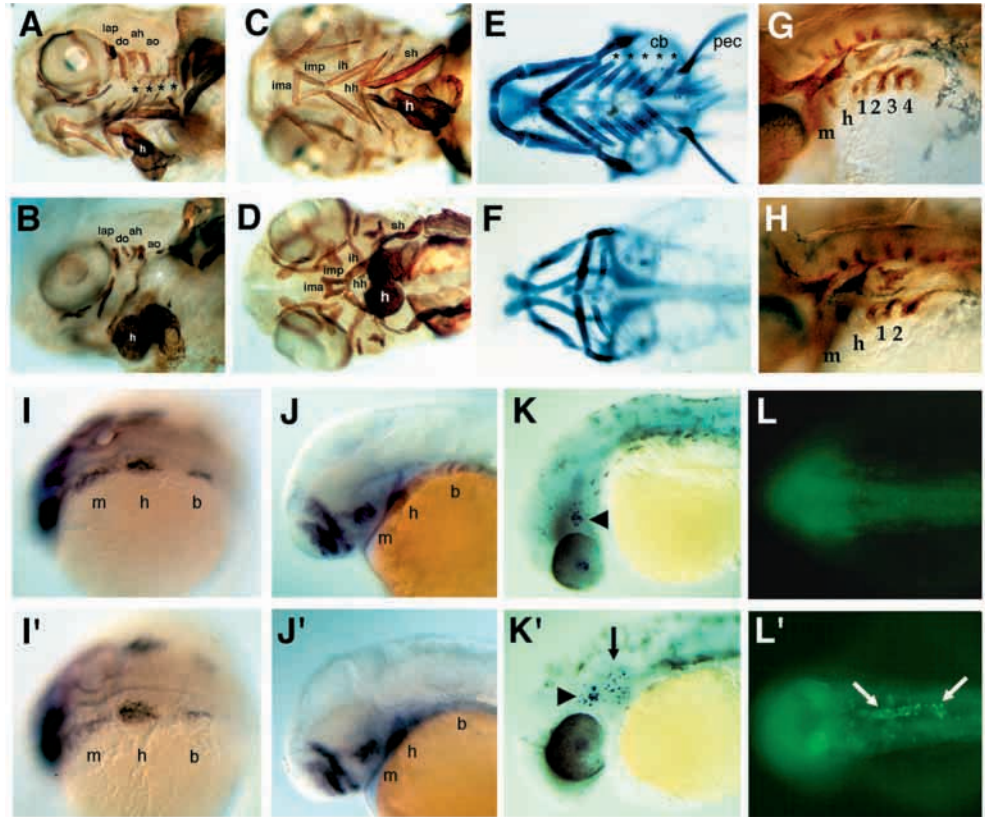
To investigate the embryonic basis of defects in the neural crest-derived cartilages of the larva, we analysed markers of both premigratory and migrating neural crest populations. We found no differences in the expression of markers of premigratory crest in *nls*, such as *snail2*, which marks most neural crest cells at 12 hpf (data not shown) or *krox20*, which marks a small group of cells that emigrate from r5 at 13 hpf (see Fig. 1H,J). In contrast, expression of *dlx2*, which marks all three migrating streams of neural crest and persists in the arch primordia, is disrupted specifically in the most posterior stream that will form the branchial cartilages. Precursors of the mandibular and hyoid arches appeared to migrate normally (Fig. 5I,I') and *dlx2*

expression in these arches appeared only slightly reduced by 40 hpf (Fig. 5J,J'). To test the possibility that the branchial neural crest cells undergo apoptotic cell death, we labelled dying cells in *nls* mutants with whole-mount TUNEL staining or Acridine Orange (Fig. 6C,D). At 24 hpf, we observed increased cell death in *nls* mutants in the anterior notochord and the third and fourth branchial arches (Fig. 5K',L'), indicating that survival of posterior branchial neural crest cells requires *nls*.

### Hindbrain defects in *nls* mutants

To investigate whether the mesodermal defects in *nls* are accompanied by defects in the neurectoderm, we examined the expression of a number of genes that mark specific AP regions of the hindbrain. Expression of *krox20*, which marks r3 and r5, is initially weaker in r5 at tailbud stage, but subsequently becomes indistinguishable from wild type (Fig. 1G–J). Expression of *valentino* (Moens et al., 1998), which marks r5/r6, is expanded by 30  $\mu$ m along the AP axis in *nls* mutants (Fig. 6A,B). Likewise, *eph-b2* expression which marks r7 (Durbin et al., 1998) is slightly expanded in *nls* as compared to wild type between 14–15 hpf (Fig. 6C,D). Thus, posterior rhombomere territories appear to be established in the appropriate locations in *nls* mutants, but are slightly enlarged relative to their wild-type counterparts. Consistent with this, we found that *hoxb3*, which in wild type is strongly expressed in a stripe that includes r5/r6, is expressed in a similar but expanded r5/r6 domain in *nls* mutants (Fig. 6E–H).

**Fig. 5.** Cartilage, muscle and neural crest defects in *nls*. (A-D) Anti-myosin immunostaining of muscles in whole-mounted wild-type (A,C) and *nls* (B,D) embryos at 3.5 days. As shown in lateral view (A,B), in wild types, both dorsal and ventral muscles of the mandibular and hyoid arches are present, but shortened in *nls*, which is clearer for the ventral muscles in ventral view (compare C with D). In branchial arches both dorsal pharyngeal wall muscles and the transverse ventral muscles (black asterisks) are absent in *nls* (white asterisk). (E,F) Alcian Blue staining of cartilages in whole-mounted wild type (E) and *nls* mutants (F) at 120 hpf, ventral views. Wild types form five ceratobranchial elements (asterisks), and in *nls* all but the first are deleted, as are the small hypobranchial and basibranchial cartilages in these segments at the midline. Note the absence of the pectoral fin skeleton (pec). (G,H) Immunostaining of branchial pouches with Zn8 antibody. Pouches 3 and 4 are absent in *nls*. Whole-mount in situ hybridisation of wild-type (I-L) and *nls* embryos (I'-L'). (I,I') Dorsolateral views of *dlx2* expression in three streams of migrating cranial neural crest in both wild type and *nls* (m, mandibular; h, hyoid; b, branchial stream). (J,J') Lateral views at 40 hpf showing *dlx2* expression in arch primordia. Expression in the branchial arches is lost in *nls*. (K,K') Lateral views at 32 hpf showing TUNEL staining of apoptotic cells in the lens and trigeminal ganglion of wild-type embryos (arrowhead), as well as in migrating neural crest cells in the branchial arches in *nls* mutants (K', arrow). (L,L') Dorsal views at 24 hpf, showing Acridine Orange staining of apoptotic cells in the anterior end of the notochord in *nls* (L', arrows). ah and ao, dorsal hyoideal muscles; cb, ceratobranchial; ima, intermandibularis anterior; imp, intermandibularis posterior; ih, interhyoideus; h, heart; hh, hyohyoideus; lap and do, dorsal mandibular muscles; sh, sternohyoideus; pec, pectoral fin.



In contrast, we found a much stronger defect in *hoxb4* expression, which in wild-type extends throughout the posterior neurectoderm up to a boundary between r6 and r7 (Prince et al., 1998a). In *nls* embryos, *hoxb4* expression cannot be detected in this region before 15-16 hpf, although it is expressed normally in the somitic mesoderm and in the tailbud (Fig. 6I,J; and not shown). By 16 hpf, however, *hoxb4* expression is established at a more or less appropriate position in the neural tube, although it does not extend caudally towards the tailbud (Fig. 6K,L).

RARs are autonomously required for the neural induction of *hoxd1* by mesodermal signals in *in vitro* conjugates from *Xenopus*, while in the chick, *Hoxb4* is a direct target of RAR $\alpha$  (Kolm et al., 1997; Gould et al., 1998). To test if the defect in *hoxb4* expression in *nls* might be due to a disruption in RAR expression, we analysed the distribution of both RAR $\alpha$  and RAR $\gamma$  mRNA (Joore et al., 1994). We detected no defects in RAR $\gamma$  in *nls* (not shown); however, RAR $\alpha$  expression is downregulated precisely in the region of the neural tube disrupted in mutants. By contrast, RAR $\alpha$  expression outside the CNS in the mesoderm appears to be slightly upregulated, and expression in the tailbud is unaffected (Fig. 6M,N). Thus, defects in RAR $\alpha$  regulation in *nls* correlate with the defects in expression of *hoxb4*.

To examine the consequences of these changes in gene

expression for neuronal patterning in the posterior hindbrain we used a combination of neuronal markers and dye labelling techniques. A subset of interneurons express *tbx-c* (Dheen et al., 1999). In *nls*, expression in these interneurons is strongly reduced at 36 hpf (Fig. 6P,R). We also retrogradely labelled the large primary reticulospinal interneurons of the hindbrain with rhodamine-dextran by injection into the spinal cord; these are variably disrupted in the caudal hindbrain of *nls* mutants (data not shown). Likewise, spinal motoneurons that innervate the pectoral fin bud are reduced in *nls*, as revealed by labelling with the Zn8 antibody (Fig. 6S,T). The loss of hindbrain interneurons, as well as neuronal subpopulations in the rostral spinal cord, correlates with the restricted defects in gene expression at this AP level, such as the failure to initiate *hoxb4* expression. Thus, neural defects are milder compared with complete loss of RA signalling, as in the *Raldh2*<sup>-/-</sup> mouse, where the caudal hindbrain is absent due to misspecification to a more rostral fate.

#### RALDH2 is required in the mesoderm for initiation of *hoxb4* expression in neural ectoderm

To determine the cellular requirement for *nls* function, we transplanted cells from embryos labelled with a lineage tracer into unlabeled hosts at the gastrula stage (Fig. 7). First, we asked if *nls* cells can contribute to tissues disrupted in the *nls*

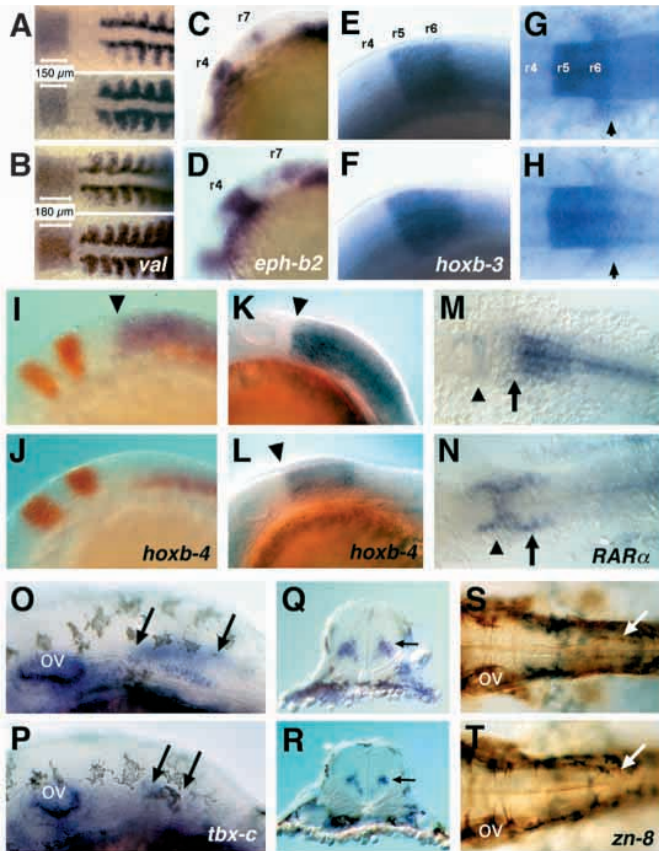


**Fig. 6.** Hindbrain patterning in wild-type and *nls* embryos. In situ hybridisation of wild type (upper panels in A,C,E,G,I,K,M,O,Q,S) and *nls* (lower panels in B,D,F,H,J,L,N,P,R,T) embryos with markers expressed in the hindbrain and spinal cord. (A,B) *valentino* expression in r5/r6 is expanded along the AP axis (see also r3-r7 in Figs 2D,F,J); *myoD* expression abuts r7 in wild type and r6 and r7 in *nls*. (C,D) Expression of *ephrin b2* appears normal in r4 and r7 in *nls*. (E-H) *hoXB3* expression in r5/r6 and in the migrating postotic neural crest (arrows in G,H). (I-L) *hoXB4* expression (blue) in the neural tube is absent in a 12 hpf *nls* embryo; *krox20* expression (red) is expanded; *myoD* (red) counterstain identifies *nls* embryos (I,J). At 16 hpf, neural *hoXB4* expression is initiated with an anterior expression boundary at r6/r7 (arrowheads), yet it is not fully expanded caudally (K,L). (M,N) *RARα* is expressed caudally to the r6/r7 boundary in the neural tube (arrows) in wild type; *nls* embryos are devoid of neural expression, while expression is unaffected or slightly elevated in more rostral regions of the neural tube (arrowheads). (O-R) *tbx-c* expression in interneurons of the anterior spinal cord (arrows) is reduced in *nls*; (Q,R) cross sections show *tbx-c* expression in the spinal cord (arrows). (S,T) Immunostaining with the Zn8 antibody of spinal cord neurones at the level of the pectoral fins (arrows) shows loss of these neurones in *nls*. ov, otic vesicle. Embryonic stages: 24 hpf in A,B,E-H; 10 somite stage in C,D; 12 hpf in I,J,M,N; 16 hpf in K,L; 33 hpf in O-T. Lateral (C-F,I-L,O,P) and dorsal (A,B,G,H,M,N,S,T) views, anterior towards the left.

mutation, such as the posterior head mesoderm, and axial, paraxial and posterior hindbrain. In an otherwise wild-type embryo, donor derived *nls* cells were found to be able to spread widely throughout the neural ectoderm of the hindbrain and anterior spinal cord (Fig. 7A,B,I; Table 4). In other cases, mutant cells readily populated regions of the paraxial (Fig. 7A') and axial (Fig. 7C) mesoderm of the head (Table 4). Likewise, transplants of wild type mesoderm into *nls* mutants were able to populate the anterior somites (Fig. 7F).

We then used such mesodermal grafts to determine whether the defects in *hoXB4* expression in the neural tube of *nls* mutants (Fig. 7D,E) might reflect defects in a non-autonomous signal from surrounding mesoderm that requires *nls/raldh2*. With reference to fate maps of head mesoderm (Kimmel et al., 1990), we transplanted mesodermal precursors from biotin-dextran labelled wild-type donors into unlabeled mutant hosts at the gastrula stage. In many cases these transplanted cells spread widely along one side of mutant host embryos and often form muscles in the anterior somites adjacent to the region in which *hoXB4* is normally expressed (Fig. 7F-H). In 71% of cases in which wild-type cells populated this region in *nls*, we observed a partial recovery of early *hoXB4* expression several hours before 15 hpf (Table 4). Control transplants of mutant mesoderm into *nls* hosts had no such effect on *hoXB4* expression (Fig. 7G). Thus,

**Fig. 7.** Induction of neural *hoXB4* expression in *nls* by transplanted wild-type somitic mesoderm.

(A-C) In a wild-type host *nls* mutant donor cells (brown) contribute to hindbrain (A), spinal cord (A,B), paraxial mesoderm (A', arrow) and notochord (C) at the head/trunk boundary. In situ hybridisation detects expression of *krox20* in the hindbrain (r3, r5) and *myoD* in somites (s1,s2). (D,E) *krox20* and *hoXB4* expression in wild type and *nls* mutants. (F-G) Fluorescent images of donor cells and bright field images of hosts after stained for expression of *krox20* and *hoXB4*; wild-type cells populating paraxial mesoderm of anterior somites and individual spinal cord neurones in a 15 hpf *nls* embryo (F); rescue of neural expression of *hoXB4* by wild-type cells (F'); *nls* cells transplanted to the anterior somitic mesoderm of a *nls* host (G) are not able to induce neural *hoXB4* expression (G'). (H) Another example of rescue of neural *hoXB4* expression by transplanted wild-type cells (brown staining) in somites of a *nls* host. Note that both sides of the neural tube are rescued in F' and H, although wild-type cells are unilaterally distributed. (I) Example of a 15 hpf *nls* embryo with a massive contribution of wild-type donor cells (brown staining) to the hindbrain and spinal cord. *HoXB4* expression is not induced in either donor or host-derived neural ectoderm. Dorsal views.

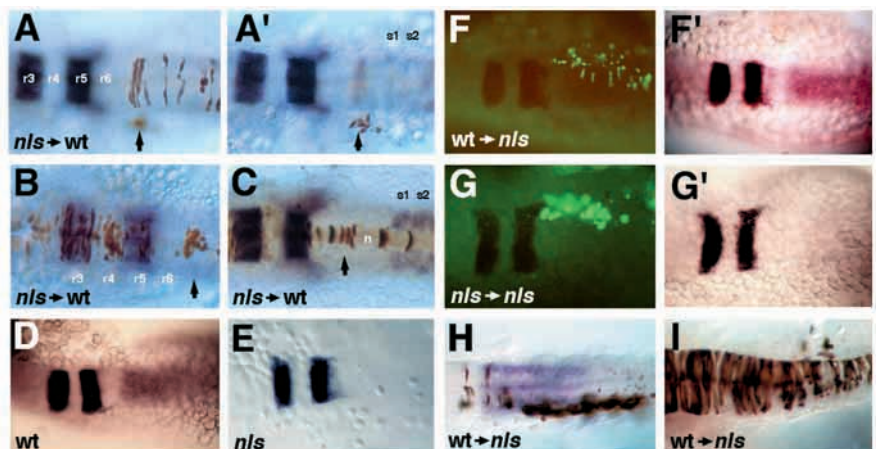


**Table 4. Fates of transplanted cells in mosaic embryos**

Transplant and sample size (n)	Phenotypes		Hoxb4 positive	Fates scored		
	Donor	Host		Somites 1-5 and head mesoderm	Neural tube	Notochord
Paraxial mesoderm (n=51)						
(n=21)	Wild type	Wild type	10/10 (100%)	10/11 (91%)	–	–
(n=14)	Wild type	<i>nls</i>	5/7 (71%)	7/7 (100%)	–	–
(n=10)	<i>nls</i>	Wild type	6/6 (100%)	4/4 (100%)	–	–
(n=6)	<i>nls</i>	<i>nls</i>	0/4 (0%)	1/2 (50%)	–	–
Axial mesoderm (n=21)						
(n=11)	Wild type	Wild type	3/3 (100%)	–	–	7/8 (88%)
(n=6)	Wild type	<i>nls</i>	0/2 (0%)	–	–	3/4 (75%)
(n=4)	<i>nls</i>	Wild type	–	–	–	4/4 (100%)
Neural ectoderm (n=33)						
(n=18)	Wild type	Wild type	6/6 (100%)	–	11/12 (92%)	–
(n=9)	Wild type	<i>nls</i>	0/4 (0%)	–	4/5 (80%)	–
(n=6)	<i>nls</i>	Wild type	2/2 (100%)	–	4/4 (100%)	–

Transplants were scored at 12–13 hpf for *hoxb4* expression by in situ hybridisation and at 24 hpf for contributions to mesodermal or neural derivatives at the head/trunk boundary.

the activity of *nls/raldh2* in paraxial mesoderm is necessary for *hoxb4* expression in the adjacent neural ectoderm.

## DISCUSSION

Using a marker-based screening strategy we have identified *nls*, a new mutation in the zebrafish that disrupts patterning along the AP axis of the embryo. Linkage analysis, together with morpholino phenocopying and phenotypic rescue by RA and *raldh2* mRNA injection, strongly suggest that a missense mutation in a conserved glycine residue of the RA metabolic enzyme RALDH2, causing a reduction in RA activity underlies the *nls* phenotype. Mutant embryos reveal a complex requirement for *nls/raldh2* in the formation of both axial and paraxial mesoderm, survival of neural crest cells and specification of cells in the hindbrain at the head/trunk boundary. By generating genetically mosaic embryos we have adduced in vivo evidence for mesodermally derived RA-dependent signals that pattern the CNS. We suggest a model in which RA production in the paraxial mesoderm underlies both short- and long-range effects of RA signalling on the head mesoderm and CNS. The model predicts a direct local role for *RARα* in *hoxb4* regulation in the neural tube in response to RA-signalling from the forming somites. In addition, it postulates a limited influence of RA signalling not only on the neural ectoderm, but also on the head mesoderm, with important secondary consequences for hindbrain and neural crest patterning.

The combination of hindbrain, neural crest and limb defects characteristic of *nls* mutant embryos is similar to that caused by targeted inactivation of *Raldh2* in the mouse (Niederreither et al., 1999), as well as by VAD in the quail (Maden et al., 1996; Gale et al., 1999) and rat (White et al., 2000) embryos. The hindbrain defects in *nls* embryos are, however, less severe than in these other cases: in both the mutant and VAD embryos, rhombomere-specific characteristics caudal to r4 are disrupted whereas in *nls*, posterior rhombomeres appear slightly expanded and only neurones near the hindbrain-spinal cord boundary are disrupted. This phenotype is reminiscent of the

milder forms of VAD in rat embryos (White et al., 2000) and of the partial rescue of *Raldh2*<sup>-/-</sup> mice by maternal application of RA (Niederreither et al., 2000), and suggests that the posterior hindbrain and anterior spinal cord are most sensitive to a reduction in RA levels.

The fact that the *nls* phenotype is closer to the effects of attenuation, rather than elimination of RA signalling in amniote embryos could be explained if the *nls*<sup>i26</sup> allele behaves as a hypomorph, the mutant protein retaining residual enzymatic activity. Against this, however, structural modelling predicts that the glycine-to-arginine substitution found in *nls*<sup>i26</sup> would result in a complete loss of activity, a view supported by our finding that *nls* is precisely phenocopied by morpholino-mediated translational inhibition of the *raldh2* gene that we have cloned. This raises the possibility that zebrafish may possess a second *raldh2* gene that can partially compensate for the loss of *nls/raldh2*, a possibility consistent with the finding that many teleost genes are duplicated (Amores et al., 1998).

### A restricted requirement for *nls/raldh2* at the head/trunk boundary

RA has been proposed to act as a graded posteriorising signal throughout the AP axis of the CNS (reviewed by Gavalas and Krumlauf, 2000). Mutation of *nls/raldh2* and reduction of RA in zebrafish through pharmacological inhibition of aldehyde dehydrogenases (Perz-Edwards et al., 2001), however, suggest that RA acts in a more localised manner. From tail bud stages onwards, *nls/raldh2* expression is confined to trunk and tail mesoderm, yet defects in *nls* are largely in the posterior head. Thus, *nls/raldh2* and, by inference, RA produced in presumptive somites may act at only a short distance and at high concentrations. Perhaps only cells in close proximity to the source of RA are able to respond, while others require different posteriorising signals, such as members of the fibroblast growth factor and Wnt families.

Defects in paraxial mesoderm in *nls/raldh2* mutants may secondarily cause its hindbrain defects through loss of local posteriorising induction (Itasaki et al., 1996). *nls* mutants lack mesoderm between the level of r5 and somite 1 at the beginning of somitogenesis, suggesting that *nls/raldh2* activity must be

required during gastrulation; this correlates well with the early zygotic expression of *nls/raldh2* in the germ ring of gastrulating embryos, which forms the mesendoderm (Kimmel et al., 1990). In VAD quail embryos, a similar defect has been accounted for by apoptosis of mesodermal cells within the first somite during a brief period in early somitogenesis (Maden et al., 1997). Such patterns of apoptosis were not observed, however, during gastrulation stages in *nls*. Moreover, the mesodermal deficiency in *nls/raldh2* occurs in a much broader region anterior to the somites, and includes both axial and paraxial cells. Our molecular analysis rules out the possibility that the posterior head mesoderm is transformed into more caudal tissues, as anterior-most somites in *nls* develop with their normal identities. RA may instead be involved in maintaining cell proliferation at the head/trunk boundary, though we currently have no direct evidence for such an effect.

Surprisingly, we find defects not only in the paraxial mesoderm of *nls*, but also in the notochord, a structure that is known to influence patterning of the overlying neural tube. Although the notochord has not been implicated specifically in AP patterning of the hindbrain, recent evidence in zebrafish has shown that some Hox genes are expressed in AP restricted domains near the head/trunk boundary (Prince et al., 1998b). *nls/raldh2* is not expressed in the notochord, suggesting that the effects on its development are non-autonomous, which is supported by our mosaic results. Our data suggest that, similar to its restricted influences on the posterior hindbrain, RA signalling from the somites acts locally on axial as well as paraxial mesoderm.

Correlated with these spatially restricted phenotypes in the mesoderm and nervous system, *nls* mutants later exhibit defects in branchial arches. Again these are confined to the posterior head and recapitulate the branchial hypoplasia in chick embryos treated with pan-RAR antagonists and in *Raldh2*-deficient mice (Niederreither et al., 1999; Wendling et al., 2000). In this case, however, *Raldh2* appears to be required for cell survival in the neural crest-derived skeleton. Crest cells are apoptotic in the pharyngeal primordia in *nls*, as they are in VAD and *Raldh2*<sup>-/-</sup> mice (Maden et al., 1996; Niederreither et al., 1999). The correlation between the loss of posterior head mesoderm and posterior arches in *nls* mutants further suggests that apoptosis may be a secondary consequence of earlier defects in posterior head mesoderm and/or endoderm. Patterning of cranial neural crest has been shown to respond to both mesenchymal-mesenchymal interactions with mesoderm, as well as epithelial-mesenchymal interactions with surrounding endoderm in the arches (Trainor and Krumlauf, 2000; Tyler and Hall, 1977). Alternatively, crest cells may require *nls/raldh2* directly for their survival, as crest cells appear to be particularly sensitive to alterations of RA levels (Ellies et al., 1997). RAR $\alpha$ /RAR $\beta$  double mutant mice have hypoplastic posterior branchial arches similar to those seen in ablations of postotic neural crest in chick embryos (Dupe et al., 1999; Ghyselinck et al., 1997), despite the normal generation and migration of crest. Thus, the developmental deficiencies observed in the pharyngeal region of *nls* are likely to be caused by local defects in postotic mesoderm and endoderm, rather than by a long-range graded requirement for RA.

Another striking aspect of the *nls* phenotype is the complete lack of pectoral fin buds. *nls/raldh2* is required early during pectoral fin induction locally in the fin field, as one of the

earliest markers of the fin field, *tbx5.1*, is not expressed in the lateral plate mesoderm in *nls* mutants. This phenotype correlates well with expression of *nls/raldh2* in this region of the mesoderm between the 6- and 12-somite stage (12-15 hpf). *raldh2* expression precedes (not shown) and is then maintained during outgrowth of the apical fold at the posterior of the pectoral fin bud (Fig. 3R). As we have shown for *hoxb4* in the neural tube, *nls/raldh2* may also be required for the expression of Hox genes in the prospective fin field, thus being involved in setting up limb position along the AP axis of the lateral plate mesoderm (Cohn et al., 1997). A common model of limb-field determination proposes a function for fibroblast growth factors (FGFs) as limb inducers and locates the source of limb inducing activity in the intermediate mesoderm (reviewed in Martin, 1998). RA induces FGF or generates competence of the flank to respond, and FGFs are capable of inducing ectopic limb buds in the lateral plate mesoderm of the chick flank. *raldh2* may thus be required for the local induction of an FGF or another inducing signal.

### The role of the mesoderm in neural patterning

A large body of evidence has previously implicated RA in mediating signals from the mesoderm to the neural tube. In *Xenopus*, tissue recombination experiments have demonstrated a requirement for RARs in the ectoderm for induction of Hox gene expression through mesoderm-derived signals (Kolm et al., 1997). Conversely, upregulation of RA during somitogenesis has been shown to be required for cultured paraxial mesoderm to induce cells of spinal cord fate, while loss of this inducing capacity by freeze-thawing paraxial cells can be restored through administration of RA (Muhr et al., 1999). In line with these data, transgenic RAR $\beta$ -*lacZ* reporter constructs (where the RA-responsive element of the RAR $\beta$ -gene has been fused to the *lacZ* reporter gene) (Balkan et al., 1992; Mendelsohn et al., 1991; Rossant et al., 1991; Zimmer, 1992), as well as similar reporter constructs in zebrafish (Marsh-Armstrong et al., 1995; Perz-Edwards et al., 2001), are activated in the neural tube. Such activation of neural RA-responsive genes can be explained by diffusion of RA from the paraxial mesoderm. While the lack of detectable *nls/raldh2* mRNA in the prospective neural tube during gastrulation and segmentation stages is highly suggestive of a non-autonomous action of RA, the results of our mosaic analyses provide the first conclusive evidence for this mode of action. Transplantation of wild-type cells into the somitic mesoderm of *nls* embryos restores early *hoxb4* expression, whereas that of *nls* cells in the same position does not. Likewise, *nls* ectodermal cells intercalate normally into a wild-type CNS in the *hoxb4*-expressing domain, suggesting that *nls/raldh2* is not required for cells to take on the identity of this region of the neural tube.

Our analysis of *hoxb4* expression in *nls* reveals that, as in the amniote embryo (Gould et al., 1998), the zebrafish *hoxb4* gene follows a biphasic mode of transcriptional regulation. The first phase establishes neural expression and depends on *raldh2* activity, while the second phase is independent of *raldh2*. These regulatory steps are linked to neural promoter elements that regulate *hoxb4* expression in chick and mouse embryos, one of which acts before rhombomere formation and one of which acts later in maintenance of expression. Activation of the early neural enhancer is mediated by RA response elements

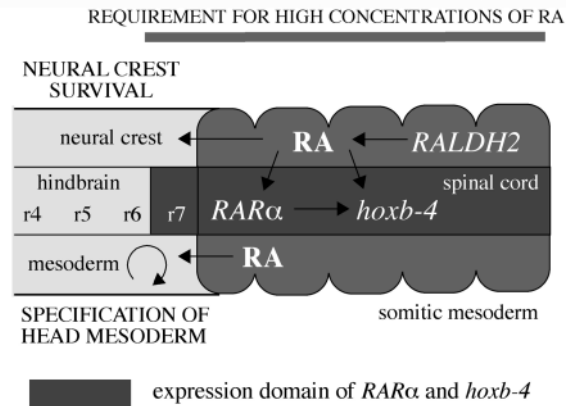


**Fig. 8.** Model for the role of *nls/raldh2* in patterning the posterior head and neural tube. High local concentrations of RA are required for patterning of posterior axial and paraxial head mesoderm, survival of posterior neural crest cells, and induction of gene expression in the neural tube. Dorsal schematic view of an idealised zebrafish embryo during early segmentation stages with anterior to the left.

(Gould et al., 1998). Our results are consistent with a similar control of *hoxb4* expression in fish: *hoxb4* is initially not expressed but recovers in *nls/raldh2* mutants after 15–16 hpf, albeit to less than its full posterior extent. The loss of hindbrain interneurons and neurons in the anterior spinal cord may result from a failure to initiate this first phase of *hoxb4* expression. Similarities in the expression of *RARα* in the neural tube (Joore et al., 1994) and dependence on *raldh2* suggests that *RARα* is likely to be a major effector of paraxial RA signalling in the neural tube. This is supported by the finding that overexpression of a dominant negative form of *Xenopus RARα1* in the avian neural tube blocks induction of *hoxb4* (Gould et al., 1998). *RARα* expression may be under autoregulatory control during this phase or may be controlled by other *RARs*, as its neural expression is dependent upon RA signalling. Similarly, *nls/raldh2* itself may be subject to a RA-mediated autoregulation within the somitic mesoderm, as its mRNA levels increase in *nls/raldh2* mutant embryos older than 30 hpf. In line with this, previous studies in chick have shown that exogenous RA represses *raldh2* expression.

Our model of short-range RA-dependent interactions between the mesoderm and neural tube (Fig. 8) based on our genetic analysis in zebrafish is consistent with earlier results obtained from experimental manipulation of the chick embryos. This model makes testable predictions and thus provides a framework for future experiments, both to explore the exact source and graded nature of the RA signal and the nature of the responses of neural cells to RA during vertebrate development.

For the generous gift of probes we thank J. Campos-Ortega, L. Durbin, T. Jowett, V. Korzh, S. Krauss, C. Moens, C. Neumann, V. Prince, S. Schulte-Merker and D. Zivkovic-Jongejans. We also thank J. Rafferty for his expert advice on structure modelling, C. E. Allen for help with rescue experiments, members of the Ingham laboratory for stimulating discussions and A. Meyer for his generous support. This work was sponsored in part through a Marie-Curie Fellowship (FMBICT960675) to G.B., a German Human Genome Project grant (DHGP grant 01KW9627/1) to R.G., an HFSP Fellowship (592 1995)

and a Wellcome Trust Career Development Fellowship (RCDF 055120) to T. S., and a TMR-Network grant (ERBFMRXCT960024) and BBSRC research grant (50/G12140) to P. W. I.

## REFERENCES

- Amores, A., Force, A., Yan, Y. L., Joly, L., Amemiya, C., Fritz, A., Ho, R. K., Langeland, J., Prince, V., Wang, Y. L. et al. (1998). Zebrafish *hox* clusters and vertebrate genome evolution. *Science* **282**, 1711–1714.
- Balkan, W., Colbert, M., Bock, C. and Linney, E. (1992). Transgenic indicator mice for studying activated retinoic acid receptors during development. *Proc. Natl. Acad. Sci. USA* **89**, 3347–3351.
- Begemann, G. and Ingham, P. W. (2000). Developmental regulation of *Tbx5* in zebrafish embryogenesis. *Mech. Dev.* **90**, 299–304.
- Berggren, K., McCaffery, P., Dräger, U. and Forehand, C. J. (1999). Differential distribution of retinoic acid synthesis in the chicken embryo as determined by immunolocalization of the retinoic acid synthetic enzyme, RALDH-2. *Dev. Biol.* **210**, 288–304.
- Blumberg, B., Bolado, J., Jr., Moreno, T. A., Kintner, C., Evans, R. M. and Papalopulu, N. (1997). An essential role for retinoid signaling in anteroposterior neural patterning. *Development* **124**, 373–379.
- Cohn, M. J., Patel, K., Krumlauf, R., Wilkinson, D. G., Clarke, J. D. and Tickle, C. (1997). *Hox9* genes and vertebrate limb specification. *Nature* **387**, 97–101.
- Colbert, M. C., Rubin, W. W., Linney, E. and LaMantia, A. S. (1995). Retinoid signaling and the generation of regional and cellular diversity in the embryonic mouse spinal cord. *Dev. Dyn.* **204**, 1–12.
- Costaridis, P., Horton, C., Zeitlinger, J., Holder, N. and Maden, M. (1996). Endogenous retinoids in the zebrafish embryo and adult. *Dev. Dyn.* **205**, 41–51.
- Currie, P. D., Schilling, T. F. and Ingham, P. W. (1999). Small-scale marker-based screening for mutations in zebrafish development. *Methods Mol. Biol.* **97**, 441–460.
- Dan-Goor, M., Silberstein, L., Kessel, M. and Muhrad, A. (1990). Localization of epitopes and functional effects of two novel monoclonal antibodies against skeletal muscle myosin. *J. Muscle Res. Cell Motil.* **11**, 216–226.
- Dheen, T., Sleptsova-Friedrich, I., Xu, Y., Clark, M., Lehrach, H., Gong, Z. and Korzh, V. (1999). Zebrafish *tbx-c* functions during formation of midline structures. *Development* **126**, 2703–2713.
- Dickman, E. D., Thaller, C. and Smith, S. M. (1997). Temporally-regulated retinoic acid depletion produces specific neural crest, ocular and nervous system defects. *Development* **124**, 3111–3121.
- Dueter, G. (2000). Families of retinoid dehydrogenases regulating vitamin A function: production of visual pigment and retinoic acid. *Eur. J. Biochem.* **267**, 4315–4324.
- Dupe, V., Davenne, M., Brocard, J., Dolle, P., Mark, M., Dierich, A., Chambon, P. and Rijli, F. M. (1997). In vivo functional analysis of the *Hoxa-1* 3' retinoic acid response element (3'RARE). *Development* **124**, 399–410.
- Dupe, V., Ghyselinck, N. B., Wendling, O., Chambon, P. and Mark, M. (1999). Key roles of retinoic acid receptors alpha and beta in the patterning of the caudal hindbrain, pharyngeal arches and otocyst in the mouse. *Development* **126**, 5051–5059.
- Durbin, L., Brennan, C., Shiomi, K., Cooke, J., Barrios, A., Shanmugalingam, S., Guthrie, B., Lindberg, R. and Holder, N. (1998). Eph signaling is required for segmentation and differentiation of the somites. *Genes Dev.* **12**, 3096–3109.
- Durston, A. J., van der Wees, J., Pijnappel, W. W. and Godsave, S. F. (1998). Retinoids and related signals in early development of the vertebrate central nervous system. *Curr. Top. Dev. Biol.* **40**, 111–175.
- Ellies, D. L., Langille, R. M., Martin, C. C., Akimenko, M. A. and Ekker, M. (1997). Specific craniofacial cartilage dysmorphogenesis coincides with a loss of *dlx* gene expression in retinoic acid-treated zebrafish embryos. *Mech. Dev.* **61**, 23–36.
- Gale, E., Zile, M. and Maden, M. (1999). Hindbrain respecification in the retinoid-deficient quail. *Mech. Dev.* **89**, 43–54.
- Gavalas, A. and Krumlauf, R. (2000). Retinoid signalling and hindbrain patterning. *Curr. Opin. Genet. Dev.* **10**, 380–386.
- Ghyselinck, N. B., Dupe, V., Dierich, A., Messaddeq, N., Garnier, J. M., Rochette-Egly, C., Chambon, P. and Mark, M. (1997). Role of the retinoic acid receptor beta (*RARβ*) during mouse development. *Int. J. Dev. Biol.* **41**, 425–447.

- Gould, A., Itasaki, N. and Krumlauf, R. (1998). Initiation of rhombomeric Hoxb4 expression requires induction by somites and a retinoid pathway. *Neuron* **21**, 39-51.
- Grapin-Botton, A., Bonnini, M. A., McNaughton, L. A., Krumlauf, R. and Le Douarin, N. M. (1995). Plasticity of transposed rhombomeres: Hox gene induction is correlated with phenotypic modifications. *Development* **121**, 2707-2721.
- Haselbeck, R. J., Hoffmann, I. and Duester, G. (1999). Distinct functions for Aldh1 and Raldh2 in the control of ligand production for embryonic retinoid signaling pathways. *Dev. Genet.* **25**, 353-364.
- Horton, C. and Maden, M. (1995). Endogenous distribution of retinoids during normal development and teratogenesis in the mouse embryo. *Dev. Dyn.* **202**, 312-323.
- Hukriede, N. A., Joly, L., Tsang, M., Miles, J., Tellis, P., Epstein, J. A., Barbazuk, W. B., Li, F. N., Paw, B., Postlethwait, J. H. et al. (1999). Radiation hybrid mapping of the zebrafish genome. *Proc. Natl. Acad. Sci. USA* **96**, 9745-9750.
- Itasaki, N., Sharpe, J., Morrison, A. and Krumlauf, R. (1996). Reprogramming Hox expression in the vertebrate hindbrain: influence of paraxial mesoderm and rhombomere transposition. *Neuron* **16**, 487-500.
- Jessell, T. M. (2000). Neuronal specification in the spinal cord: inductive signals and transcriptional codes. *Nat. Rev. Genet.* **1**, 20-29.
- Joore, J., van der Lans, G. B., Lanser, P. H., Vervaart, J. M., Zivkovic, D., Speksnijder, J. E. and Kruijer, W. (1994). Effects of retinoic acid on the expression of retinoic acid receptors during zebrafish embryogenesis. *Mech. Dev.* **46**, 137-150.
- Kastner, P., Grondona, J. M., Mark, M., Gansmuller, A., LeMeur, M., Decimo, D., Vonesch, J. L., Dolle, P. and Chambon, P. (1994). Genetic analysis of RXR alpha developmental function: convergence of RXR and RAR signaling pathways in heart and eye morphogenesis. *Cell* **78**, 987-1003.
- Kastner, P., Mark, M., Ghyselink, N., Krezel, W., Dupe, V., Grondona, J. M. and Chambon, P. (1997). Genetic evidence that the retinoid signal is transduced by heterodimeric RXR/RAR functional units during mouse development. *Development* **124**, 313-326.
- Kimmel, C. B., Warga, R. M. and Schilling, T. F. (1990). Origin and organization of the zebrafish fate map. *Development* **108**, 581-594.
- Kimmel, C. B., Ballard, W. W., Kimmel, S. R., Ullmann, B. and Schilling, T. F. (1995). Stages of embryonic development of the zebrafish. *Dev. Dyn.* **203**, 253-310.
- Kolm, P. J., Apekin, V. and Sive, H. (1997). Xenopus hindbrain patterning requires retinoid signaling. *Dev. Biol.* **192**, 1-16.
- Krauss, S., Maden, M., Holder, N. and Wilson, S. W. (1992). Zebrafish pax[b] is involved in the formation of the midbrain-hindbrain boundary. *Nature* **360**, 87-89.
- Krauss, S., Concordet, J. P. and Ingham, P. W. (1993). A functionally conserved homolog of the Drosophila segment polarity gene hh is expressed in tissues with polarizing activity in zebrafish embryos. *Cell* **75**, 1431-1444.
- Lamb, A. L. and Newcomer, M. E. (1999). The structure of retinal dehydrogenase type II at 2.7 Å resolution: implications for retinal specificity. *Biochemistry* **38**, 6003-6011.
- Maden, M., Gale, E., Kostetskii, I. and Zile, M. (1996). Vitamin A-deficient quail embryos have half a hindbrain and other neural defects. *Curr. Biol.* **6**, 417-426.
- Maden, M., Graham, A., Gale, E., Rollinson, C. and Zile, M. (1997). Positional apoptosis during vertebrate CNS development in the absence of endogenous retinoids. *Development* **124**, 2799-2805.
- Maden, M., Sonneveld, E., van der Saag, P. T. and Gale, E. (1998). The distribution of endogenous retinoic acid in the chick embryo: implications for developmental mechanisms. *Development* **125**, 4133-4144.
- Maden, M., Graham, A., Zile, M. and Gale, E. (2000). Abnormalities of somite development in the absence of retinoic acid. *Int. J. Dev. Biol.* **44**, 151-159.
- Mangelsdorf, D. J., Thummel, C., Beato, M., Herrlich, P., Schutz, G., Umesono, K., Blumberg, B., Kastner, P., Mark, M., Chambon, P. et al. (1995). The nuclear receptor superfamily: the second decade. *Cell* **83**, 835-839.
- Marsh-Armstrong, N., McCaffery, P., Hyatt, G., Alonso, L., Dowling, J. E., Gilbert, W. and Dräger, U. C. (1995). Retinoic acid in the anteroposterior patterning of the zebrafish trunk. *Roux's Arch. Dev. Biol.* **205**, 103-113.
- Marshall, H., Studer, M., Popperl, H., Aparicio, S., Kuroiwa, A., Brenner, S. and Krumlauf, R. (1994). A conserved retinoic acid response element required for early expression of the homeobox gene Hoxb-1. *Nature* **370**, 567-571.
- Martin, G. R. (1998). The roles of FGFs in the early development of vertebrate limbs. *Genes Dev.* **12**, 1571-1586.
- Mendelsohn, C., Ruberte, E., LeMeur, M., Morriss-Kay, G. and Chambon, P. (1991). Developmental analysis of the retinoic acid-inducible RAR-beta 2 promoter in transgenic animals. *Development* **113**, 723-734.
- Moens, C. B., Cordes, S. P., Giorgianni, M. W., Barsh, G. S. and Kimmel, C. B. (1998). Equivalence in the genetic control of hindbrain segmentation in fish and mouse. *Development* **125**, 381-391.
- Molgen, A., Wright, C. V., Bremiller, R., De Robertis, E. M. and Kimmel, C. B. (1990). Expression of a homeobox gene product in normal and mutant zebrafish embryos: evolution of the tetrapod body plan. *Development* **109**, 279-288.
- Morrison, A., Moroni, M. C., Ariza-McNaughton, L., Krumlauf, R. and Mavilio, F. (1996). In vitro and transgenic analysis of a human HOXD4 retinoid-responsive enhancer. *Development* **122**, 1895-1907.
- Morriss-Kay, G. M. and Sokolova, N. (1996). Embryonic development and pattern formation. *FASEB J.* **10**, 961-968.
- Muhr, J., Graziano, E., Wilson, S., Jessell, T. M. and Edlund, T. (1999). Convergent inductive signals specify midbrain, hindbrain, and spinal cord identity in gastrula stage chick embryos. *Neuron* **23**, 689-702.
- Mullins, M. C., Hammerschmidt, M., Haffter, P. and Nusslein-Volhard, C. (1994). Large-scale mutagenesis in the zebrafish: in search of genes controlling development in a vertebrate. *Curr. Biol.* **4**, 189-202.
- Niederreither, K., McCaffery, P., Dräger, U. C., Chambon, P. and Dolle, P. (1997). Restricted expression and retinoic acid-induced downregulation of the retinaldehyde dehydrogenase type 2 (RALDH-2) gene during mouse development. *Mech. Dev.* **62**, 67-78.
- Niederreither, K., Subbarayan, V., Dolle, P. and Chambon, P. (1999). Embryonic retinoic acid synthesis is essential for early mouse post-implantation development. *Nat. Genet.* **21**, 444-448.
- Niederreither, K., Vermot, J., Schuhbauer, B., Chambon, P. and Dolle, P. (2000). Retinoic acid synthesis and hindbrain patterning in the mouse embryo. *Development* **127**, 75-85.
- Noden, D. M. (1983). The embryonic origins of avian cephalic and cervical muscles and associated connective tissues. *Am. J. Anat.* **168**, 257-276.
- Oxtoby, E. and Jowett, T. (1993). Cloning of the zebrafish krox-20 gene (krx-20) and its expression during hindbrain development. *Nucleic Acids Res.* **21**, 1087-1095.
- Perozich, J., Nicholas, H., Wang, B. C., Lindahl, R. and Hempel, J. (1999). Relationships within the aldehyde dehydrogenase extended family. *Protein Sci.* **8**, 137-146.
- Perz-Edwards, A., Hardison, N. L. and Linney, E. (2001). Retinoic acid-mediated gene expression in transgenic reporter zebrafish. *Dev. Biol.* **229**, 89-101.
- Prince, V. E., Moens, C. B., Kimmel, C. B. and Ho, R. K. (1998a). Zebrafish hox genes: expression in the hindbrain region of wild-type and mutants of the segmentation gene, valentino. *Development* **125**, 393-406.
- Prince, V. E., Price, A. L. and Ho, R. K. (1998b). Hox gene expression reveals regionalization along the anteroposterior axis of the zebrafish notochord. *Dev. Genes Evol.* **208**, 517-522.
- Rossant, J., Zirngibl, R., Cado, D., Shago, M. and Giguere, V. (1991). Expression of a retinoic acid response element-hsplacZ transgene defines specific domains of transcriptional activity during mouse embryogenesis. *Genes Dev.* **5**, 1333-1344.
- Schilling, T. F. and Kimmel, C. B. (1994). Segment and cell type lineage restrictions during pharyngeal arch development in the zebrafish embryo. *Development* **120**, 483-494.
- Schilling, T. F. and Kimmel, C. B. (1997). Musculoskeletal patterning in the pharyngeal segments of the zebrafish embryo. *Development* **124**, 2945-2960.
- Schilling, T. F., Walker, C. and Kimmel, C. B. (1996). The chinless mutation and neural crest cell interactions in zebrafish jaw development. *Development* **122**, 1417-1426.
- Schulte-Merker, S., van Eeden, F. J., Halpern, M. E., Kimmel, C. B. and Nusslein-Volhard, C. (1994). no tail (ntl) is the zebrafish homologue of the mouse T (Brachyury) gene. *Development* **120**, 1009-1015.
- Solnica-Krezel, L., Schier, A. F. and Driever, W. (1994). Efficient recovery of ENU-induced mutations from the zebrafish germline. *Genetics* **136**, 1401-1420.
- Stern, C. D., Jaques, K. F., Lim, T. M., Fraser, S. E. and Keynes, R. J. (1991). Segmental lineage restrictions in the chick embryo spinal cord depend on the adjacent somites. *Development* **113**, 239-244.

- Stern, C.D. and Foley, A.C.** (1998). Molecular dissection of Hox gene induction and maintenance in the hindbrain. *Cell* **94**, 143-145.
- Studer, M., Gavalas, A., Marshall, H., Ariza-McNaughton, L., Rijli, F. M., Chambon, P. and Krumlauf, R.** (1998). Genetic interactions between Hox1 and Hoxb1 reveal new roles in regulation of early hindbrain patterning. *Development* **125**, 1025-1036.
- Swindell, E. C., Thaller, C., Sockanathan, S., Petkovich, M., Jessell, T. M. and Eichele, G.** (1999). Complementary domains of retinoic acid production and degradation in the early chick embryo. *Dev. Biol.* **216**, 282-296.
- Tada, M. and Smith, J. C.** (2000). Xwnt11 is a target of xenopus brachyury: regulation of gastrulation movements via dishevelled, but not through the canonical wnt pathway. *Development* **127**, 2227-2238.
- Trainor, P. and Krumlauf, R.** (2000). Plasticity in mouse neural crest cells reveals a new patterning role for cranial mesoderm. *Nat. Cell Biol.* **2**, 96-102.
- Trevarrow, B., Marks, D. L. and Kimmel, C. B.** (1990). Organization of hindbrain segments in the zebrafish embryo. *Neuron* **4**, 669-679.
- Tyler, M. S. and Hall, B. K.** (1977). Epithelial influences on skeletogenesis in the mandible of the embryonic chick. *Anat. Rec.* **188**, 229-239.
- van der Wees, J., Schilthuis, J. G., Koster, C. H., Diesveld-Schipper, H., Folkers, G. E., van der Saag, P. T., Dawson, M. I., Shudo, K., van der Burg, B. and Durston, A. J.** (1998). Inhibition of retinoic acid receptor-mediated signalling alters positional identity in the developing hindbrain. *Development* **125**, 545-556.
- Wang, X., Penzes, P. and Napoli, J. L.** (1996). Cloning of a cDNA encoding an aldehyde dehydrogenase and its expression in *Escherichia coli*. Recognition of retinal as substrate. *J. Biol. Chem.* **271**, 16288-16293.
- Weinberg, E. S., Allende, M. L., Kelly, C. S., Abdelhamid, A., Murakami, T., Andermann, P., Doerre, O. G., Grunwald, D. J. and Riggleman, B.** (1996). Developmental regulation of zebrafish MyoD in wild-type, no tail and spadetail embryos. *Development* **122**, 271-280.
- Wendling, O., Dennefeld, C., Chambon, P. and Mark, M.** (2000). Retinoid signaling is essential for patterning the endoderm of the third and fourth pharyngeal arches. *Development* **127**, 1553-1562.
- Westerfield, M.** (1995). *The Zebrafish Book. Guide For the Laboratory use of Zebrafish* (Danio rerio). Eugene, OR: University of Oregon Press.
- White, J. C., Shankar, V. N., Highland, M., Epstein, M. L., DeLuca, H. F. and Clagett-Dame, M.** (1998). Defects in embryonic hindbrain development and fetal resorption resulting from vitamin A deficiency in the rat are prevented by feeding pharmacological levels of all-trans-retinoic acid. *Proc. Natl. Acad. Sci. USA* **95**, 13459-13464.
- White, J. C., Highland, M., Kaiser, M. and Clagett-Dame, M.** (2000). Vitamin A deficiency results in the dose-dependent acquisition of anterior character and shortening of the caudal hindbrain of the rat embryo. *Dev. Biol.* **220**, 263-284.
- Williams, J. A., Barrios, A., Gatchalian, C., Rubin, L., Wilson, S. W. and Holder, N.** (2000). Programmed cell death in zebrafish rohn beard neurons is influenced by TrkC1/NT-3 signaling. *Dev. Biol.* **226**, 220-230.
- Zhao, D., McCaffery, P., Ivins, K. J., Neve, R. L., Hogan, P., Chin, W. W. and Dräger, U. C.** (1996). Molecular identification of a major retinoic-acid-synthesizing enzyme, a retinaldehyde-specific dehydrogenase. *Eur. J. Biochem.* **240**, 15-22.
- Zimmer, A.** (1992). Induction of a RAR beta 2-lacZ transgene by retinoic acid reflects the neuromeric organization of the central nervous system. *Development* **116**, 977-983.